Fragmentation modes and the evolution of life cycles

Yuriy Pichugin[1], Jorge Peña[1,2], Paul B. Rainey[1,3,4], and Arne Traulsen[1]

[1]Max Planck Institute for Evolutionary Biology, August-Thienemann-Str. 2, 24306 Plön, Germany

[2]GEOMAR Helmholtz Centre for Ocean Research Kiel, Evolutionary Ecology of Marine Fishes, Düsternbrooker Weg 20, 24105 Kiel, Germany

[3]Ecole Supérieure de Physique et de Chimie Industrielles de la Ville de Paris (ESPCI ParisTech), CNRS UMR 8231, PSL Research University, 75231 Paris Cedex 05, France

[4]New Zealand Institute for Advanced Study, Massey University, Private Bag 102904, Auckland 0745, New Zealand

March 24, 2017

Abstract

Reproduction is a defining feature of living systems. Reproduction modes range from binary fission in bacteria to various modes of collective-level reproduction in multicellular organisms. However, the evolution of these modes and their adaptive significance is unclear. We develop a model in which groups arise from the division of single cells that do not separate, but stay together until the moment of group fragmentation. Fragmentation occurs via either complete or partial fission, resulting in a wide range of life cycles. By determining the relationship between life cycle and population growth rate, we define optimal fragmentation modes that have a surprisingly narrow class of solutions. Our model and results provide a framework for analysing the evolution of simple life cycles and for testing the adaptive significance of different modes of reproduction.

1 Introduction

A requirement for evolution – and a defining feature of life – is reproduction [Godfrey-Smith, 2009, Libby and Rainey, 2013, Hammerschmidt et al., 2014]. Perhaps the simplest mode of reproduction is

binary fission in unicellular bacteria, whereby a single cell divides and produces two offspring cells. However, even a process as simple as this can underlie more complex modes of reproduction involving life cycles comprised of recurring collective phases, or collective phases alternating with single cell phases [Angert, 2005]. For example, in the bacterium *Neisseria*, a diplococcus, two daughter cells remain attached forming a two-celled group that separates into two groups of two cells only after a further round of cell division [Westling-Häggström et al., 1977]. *Staphylococcus aureus*, another coccoid bacterium, divides in three planes at right angles to one another to produce grape-like clusters of about 20 cells from which single cells separate to form new clusters [Koyama et al., 1977].

These are just a few examples of a large number of diverse "unicellular" reproduction modes, but why should there be such a range of life cycles? Do these reproduction modes have adaptive significance or are they simply the unintended consequences of particular cellular processes underpinning cell division? If adaptive, what selective forces shape their evolution? Do different life cycles provide different opportunities to maximise intrinsic cell growth rate, or are collectives themselves the focal units of selection?

A starting point to answer these questions is to consider benefits and costs of group membership. Benefits may arise for various reasons. Cells within groups may be better able to withstand environmental stress [de la Fuente-Núñez et al., 2013], escape predation [Boraas et al., 1998], or occupy new niches [Bonner, 1982, Rainey and De Monte, 2014]. Also, via density dependent modes of gene regulation, cells within groups may gain more of a limiting resource than they would if alone [Williams et al., 1992, Diggle et al., 2007]. On the other hand, cells within groups experience increased competition and must also contend with the build up of potentially toxic waste metabolites [Groebe and Mueller-Klieser, 1996, Stewart and Franklin, 2008]. Thus, it is reasonable to expect an optimal relationship between group size and mode of reproduction that is environment and organism dependent [Tarnita et al., 2013, Rashidi et al., 2015, Kaveh et al., 2016].

Here we formulate and study a matrix population model [Caswell, 2001] representing a population of groups of different size to consider all possible modes of group fragmentation. By determining the relationship between life cycle and population growth rate, we show that there is, overall, a narrow class of optimal modes of fragmentation. When the process of fragmentation does not involve costs, optimal fragmentation modes are characterised by a deterministic schedule and binary splitting, whereby groups fragment into exactly two offspring groups. Contrastingly, when a cost is associated

with fragmentation, it can be optimal for a group to fragment into multiple propagules of equal size.

Our results show that the range of life cycles observed in simple microbial populations are likely shaped by selection for intrinsic growth rate advantages inherent in different modes of group reproduction. These findings also have relevance for understanding the emergence of life cycles underpinning the evolution of multicellular life.

2 Methods

2.1 Group formation and fragmentation

We consider a population in which a single type of cell (or unit or individual) can form groups (or complexes or aggregates) of increasing size by cells staying together after reproduction [Tarnita et al., 2013]. We assume that the size of any group is smaller than n, and denote groups of size j by X_j. Groups die at rate d_j and cells within groups divide at rate b_j; hence groups grow at rate jb_j (Fig. 1.*a*). The vectors of birth rates $\mathbf{b} = (b_1, \ldots, b_{n-1})$ and of death rates $\mathbf{d} = (d_1, \ldots, b_{n-1})$ make the costs and benefits associated to the size of the groups explicit, thus defining the "fitness landscape" $\{\mathbf{b}, \mathbf{d}\}$ of our model.

Groups produce new complexes by fragmenting (or splitting), i.e., by dividing into smaller groups (Fig. 1.*b*). We further assume that fragmentation is triggered by the growth of individual cells within a given group. Consider a group of size j growing into a group of size $j + 1$. Such a group can either stay together or fragment. If it fragments, it can do so in one of several ways. For example, a group of size 4 can give rise to the following five "fragmentation patterns": 4 (the group does not split but stays together), 3+1 (the group splits into two offspring groups: one of size 3, and one of size 1), 2+2 (the group splits into two groups of size 2), 2+1+1 (the group splits into one group of size 2 and two groups of size 1), and 1+1+1+1 (the group splits into four cells). Mathematically, such fragmentation patterns correspond to the five partitions of 4 (a partition of a positive integer j is a way of writing j as a sum of positive integers without regard to order; the summands are called parts [Andrews, 1998]). We use the notation $\kappa \vdash \ell$ to indicate that κ is a partition of ℓ, for example $2 + 2 \vdash 4$. The number of partitions of ℓ is given by ζ_ℓ, e.g., there are $\zeta_4 = 5$ partitions of 4.

We consider a vast space of life cycles comprising all possible ways groups can grow and fragment into smaller groups. A "life cycle" (or "fragmentation mode") assigns a probability q_κ to each possible

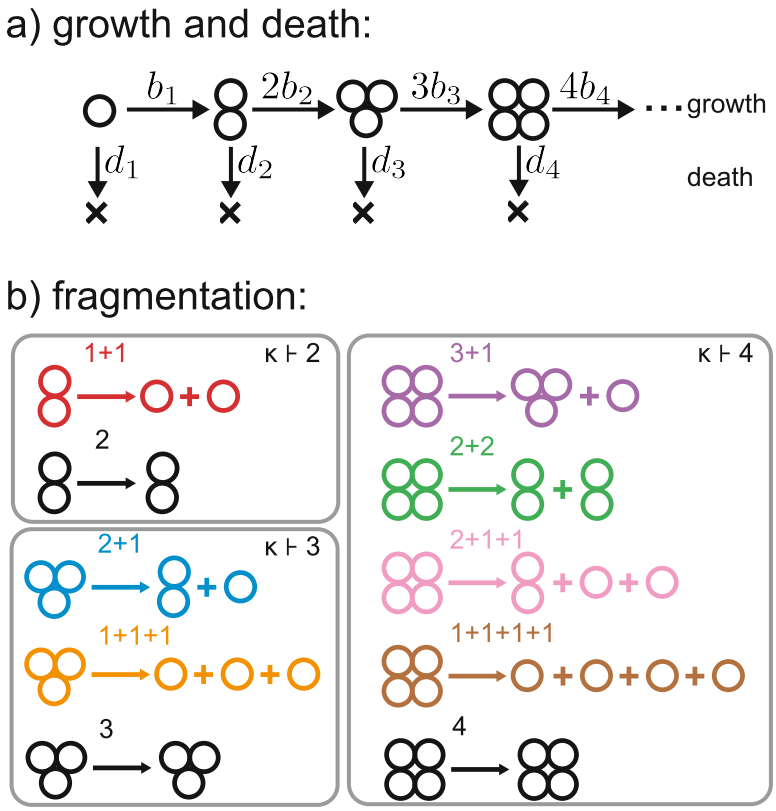

Figure 1: **Demographic dynamics depend on the growth, death, and fragmentation of groups.** *(a)* Groups of size i die at rate d_i and cells within them divide at rate b_i, hence groups grow at rate ib_i. *(b)* Fragmentation of groups occurs immediately after the reproduction of cells. Here we show all possible fragmentation patterns of groups of size $i = 2, 3, 4$. Each fragmentation pattern (determining the number and size of offspring groups) can be identified with a partition of i, i.e., a way of writing i as a sum of positive integers, that we denote by $\kappa \vdash i$. The last fragmentation pattern is i itself, in this case there is no actual fragmentation and cells stay together after individual reproduction.

fragmentation pattern (or partition) $\kappa \vdash 2$, $\kappa \vdash 3$, ..., $\kappa \vdash n$. Such probabilities satisfy $\sum_{\kappa \vdash j+1} q_\kappa = 1$ for $j = 1, \ldots, n-1$, i.e., when growing from size j to $j+1$ one of the partitions $\kappa \vdash j+1$ (including staying together without splitting, $\kappa = (j+1)$) will certainly occur. Additionally, we impose $q_n = 0$ so that, when growing from size $n-1$ to size n, a group can no longer stay together and will necessarily fragment. It follows that a given life cycle or fragmentation mode can be represented by a set of vectors of the form

$$\mathbf{q} = \left\{ (\underbrace{q_2, q_{1+1}}_{\kappa \vdash 2}), (\underbrace{q_3, q_{2+1}, q_{1+1+1}}_{\kappa \vdash 3}), \ldots, (\underbrace{q_n, q_{n-1+1}, q_{n-2+2}, \ldots, q_{1+1+\ldots+1}}_{\kappa \vdash n}) \right\}. \tag{1}$$

As an illustration, consider the subset of stochastic strategies so that (i) with probability q a two-cell group grows to size three and then fragments according to fragmentation pattern 2+1, and (ii) with probability $1-q$ a two-cell group fragments according to fragmentation pattern 1+1. Such a set of strategies is represented by

$$\mathbf{q} = \{(q_2, q_{1+1}), (q_3, q_{2+1}, q_{1+1+1})\} = \{(q, 1-q), (0, 1, 0)\}. \tag{2}$$

We consider both deterministic and stochastic life cycles. For deterministic life cycles, splitting probabilities q_κ are either zero or one, so that only one fragmentation pattern with more than one offspring group occurs. This pattern can then be used to refer to the deterministic life cycle. For example, we represent the fragmentation mode $\{(1,0), (0,1,0)\}$ by 2+1. The total number of deterministic fragmentation modes is

$$\sum_{j=1}^{n-1} (\zeta_{j+1} - 1), \tag{3}$$

which grows quickly with n: There are 128 deterministic fragmentation modes for $n = 10$, but 1295920 for $n = 50$. The more general stochastic life cycles are characterised by some fragmentation pattern occuring with a probability between zero and one (Fig. 2).

2.2 Biological reactions and demographic dynamics

Together with the fitness landscape given by the vectors of birth rates $\mathbf{b}$ and death rates $\mathbf{d}$, each fragmentation mode specifies a set of biological reactions. A number $n-1$ of reactions, of the type

$$X_i \xrightarrow{d_i} 0 \tag{4}$$

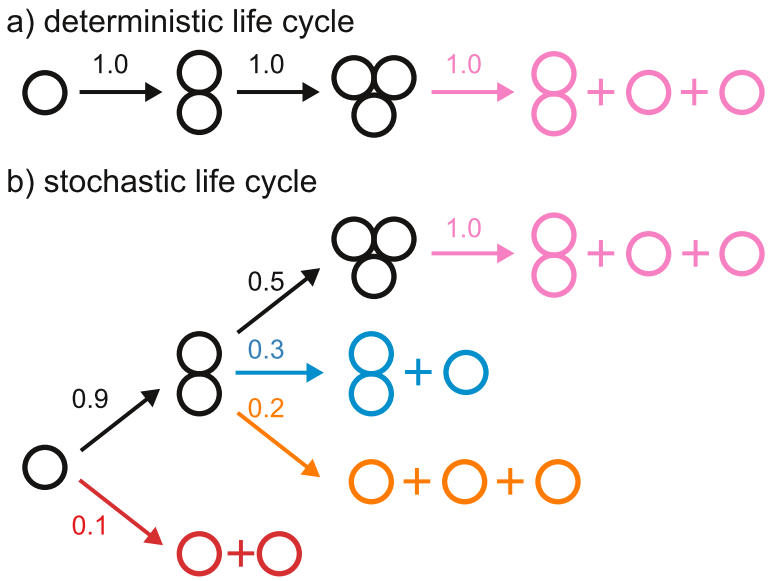

Figure 2: **Deterministic and stochastic life cycles.** *(a)* A deterministic life cycle (or fragmentation mode) given by $\mathbf{q} = \{(1,0),(1,0,0),(0,0,0,1,0)\}$, whereby groups grow to size 3 and then split according to the fragmentation pattern 2+1+1. In a deterministic life cycle, fragmentation patterns are assigned a probability equal to either zero or one, so that fragmentation occurs only at a given group size (here, 3). *(b)* A stochastic life cycle given by $\mathbf{q} = \{(0.9,0.1),(0.5,0.3,0.2),(0,0,0,1,0)\}$. In a stochastic life cycle, the probability of at least one fragmentation pattern is between zero and one.

model the death of groups; these are independent of the fragmentation mode. An additional number of reactions, one per each non-zero element of the vector $\mathbf{q}$, models the birth of units and the growth or fragmentation of groups. These reactions are of the type

$$X_j \xrightarrow{jb_j q_\kappa} \sum_{\ell=1}^{j+1} \pi_\ell(\kappa) X_\ell, \tag{5}$$

whereby a group of size j turns into a group of size $j+1$ at rate jb_j, and then instantly divides with probability q_κ into offspring groups in a way described by fragmentation pattern $\kappa \vdash j+1$, where parts equal to ℓ appear a number $\pi_\ell(\kappa)$ of times. These reactions depend on the life cycle, which specifies the probabilities of fragmentation patterns. For instance, the reaction

$$X_3 \xrightarrow{3b_3 q_{2+1+1}} X_2 + 2X_1,$$

stipulates that groups of size 3, which grow to size 4 at rate $3b_3$, will split with probability q_{2+1+1} into one group of size 2 and two groups of size 1. The growth of a group without fragmentation is also incorporated in the set of reactions given by (5). For instance, the reaction

$$X_3 \xrightarrow{3b_3 q_4} X_4,$$

stipulates that groups of size 3, which grow to size 4 at rate $3b_3$, will not split with probability q_4.

The sets of reactions (4) and (5) give rise to the system of differential equations

$$\dot{x_i} = \sum_{j=1}^{n-1} \sum_{\kappa \vdash j+1} q_\kappa \pi_i(\kappa) j b_j x_j - i b_i x_i - d_i x_i, \; i = 1, 2, \ldots, n-1, \tag{6}$$

where x_i denotes the abundance of groups of size i. This is linear system can be represented in matrix form as

$$\dot{\mathbf{x}} = \mathbf{A}\mathbf{x}, \tag{7}$$

where $\mathbf{x} = (x_1, x_2, \ldots, x_{n-1})$ is the vector of abundances of the groups of different size and

$$\mathbf{A} = \begin{pmatrix} b_1 \sum_{\kappa\vdash 2} q_\kappa \pi_1(\kappa) - b_1 - d_1 & 2b_2 \sum_{\kappa\vdash 3} q_\kappa \pi_1(\kappa) & \cdots & (n-1)b_{n-1} \sum_{\kappa\vdash n} q_\kappa \pi_1(\kappa) \\ b_1 \sum_{\kappa\vdash 2} q_\kappa \pi_2(\kappa) & 2b_2 \sum_{\kappa\vdash 3} q_\kappa \pi_2(\kappa) - 2b_2 - d_2 & \cdots & (n-1)b_{n-1} \sum_{\kappa\vdash n} q_\kappa \pi_2(\kappa) \\ 0 & 2b_2 \sum_{\kappa\vdash 3} q_\kappa \pi_3(\kappa) & \cdots & (n-1)b_{n-1} \sum_{\kappa\vdash n} q_\kappa \pi_3(\kappa) \\ 0 & 0 & \cdots & (n-1)b_{n-1} \sum_{\kappa\vdash n} q_\kappa \pi_4(\kappa) \\ \vdots & \vdots & \ddots & \vdots \\ 0 & 0 & \cdots & (n-1)b_{n-1} \sum_{\kappa\vdash n} q_\kappa \pi_{n-1}(\kappa) - (n-1)b_{n-1} - d_{n-1} \end{pmatrix} \tag{8}$$

is the projection matrix determining the demographic dynamics of the population.

Note that the entries of the projection matrix $\mathbf{A}$ are functions of the life cycle $\mathbf{q}$ and the birth and death rates $\mathbf{b}$ and $\mathbf{d}$. Since complexes can only split into complexes of equal or smaller size, $\pi_i(\kappa) = 0$ for all $\kappa \vdash j+1$ and $i > j+1$. Hence, the projection matrix $\mathbf{A}$ has zero entries below the first subdiagonal. As an illustration, consider the subset of stochastic strategies represented by Eq. (2) and subject to the fitness landscape $\{\mathbf{b}, \mathbf{d}\} = \{(b_1, b_2), (d_1, d_2)\}$. In this simple case the projection matrix reduces to

$$\mathbf{A} = \begin{pmatrix} b_1 2(1-q) - b_1 - d_1 & 2b_2 \\ b_1 q & -d_2 \end{pmatrix}. \tag{9}$$

2.3 Population growth rate

For any life cycle $\mathbf{q}$ and any fitness landscape $\{\mathbf{b}, \mathbf{d}\}$, the projection matrix $\mathbf{A}$ is essentially non-negative, i.e., all the elements outside the main diagonal are non-negative [Cohen, 1981]. This implies that $\mathbf{A}$ has a real leading eigenvalue λ_1 with associated non-negative left and right eigenvectors $\mathbf{v}$ and $\mathbf{w}$. In the long term, the solution of Eq. (7) converges to that of an exponentially growing population with a stable distribution, i.e.,

$$\lim_{t\to\infty} \mathbf{x}(t) = e^{\lambda_1 t}\mathbf{w}.$$

The leading eigenvalue λ_1 hence gives the total population growth rate in the long term, and its associated right eigenvector $\mathbf{w} = (w_1, \ldots, w_n)$ gives the stable distribution of group sizes so that, in the long term, the fraction of complexes X_i in the population is proportional to w_i. The leading eigenvalue λ_1 is the largest solution of the characteristic equation $\det(\mathbf{A} - \lambda\mathbf{I}) = 0$. For example, the stochastic strategy represented by Eq. (2) and characterised by projection matrix (9) achieves a growth rate given by

$$\lambda_1 = \frac{b_1(1-2q) - (d_1+d_2) + \sqrt{(d_1+d_2-(1-2q)b_1)^2 + 4b_1(2qb_2 + (1-2q)d_2)}}{2}. \tag{10}$$

In the particular case of a deterministic life cycle associated to fragmentation pattern $\kappa \vdash m$, the characteristic equation reduces to (Appendix A.1)

$$F_m(\lambda) - \sum_{i=1}^{m-1} \pi_i(\kappa) F_i(\lambda) = 0, \tag{11}$$

where

$$F_i(\lambda) = \prod_{j=1}^{i-1} \left(1 + \frac{d_j + \lambda}{j b_j}\right). \tag{12}$$

For instance, the growth rate of fragmentation mode 2+1+1 (illustrated in Fig. 2*a*) is given implicitly by the largest solution of $F_4(\lambda)-F_2(\lambda)-2F_1(\lambda)=0$. As Eq. (11) is a polynomial equation of degree $m-1$, explicit formulas for the growth rate in terms of birth rates and death rates are only available for small m ($m \leq 5$). For instance, the growth rate of fragmentation modes 1+1, 1+1+1, and 2+1 are respectively given by

$$\lambda_1^{1+1} = b_1 - d_1, \tag{13a}$$

$$\lambda_1^{2+1} = \frac{-(b_1+d_1+d_2)+\sqrt{(b_1+d_1-d_2)^2+8b_1b_2}}{2}, \tag{13b}$$

$$\lambda_1^{1+1+1} = \frac{-(b_1+2b_2+d_1+d_2)+\sqrt{b_1^2+2b_1(10b_2+d_1-d_2)+(2b_2-d_1+d_2)^2}}{2}. \tag{13c}$$

For larger values of m, we solve Eq. (11) numerically.

2.4 Dominance and optimality

For a given fitness landscape $\{\mathbf{b},\mathbf{d}\}$, we can take the leading eigenvalue $\lambda_1(\mathbf{q};\mathbf{b},\mathbf{d})$ as a measure of fitness of life cycle $\mathbf{q}$, and consider the competition between two different life cycles, $\mathbf{q}_1$ and $\mathbf{q}_2$. Indeed, under the assumption of no density limitation, the evolutionary dynamics are described by two uncoupled sets of differential equations of the form (7): one set for $\mathbf{q}_1$ and one set for $\mathbf{q}_2$. In the long term, $\mathbf{q}_1$ outcompetes $\mathbf{q}_2$ if $\lambda_1(\mathbf{q}_1;\mathbf{b},\mathbf{d}) \geq \lambda_1(\mathbf{q}_2;\mathbf{b},\mathbf{d})$; we then say that life cycle $\mathbf{q}_1$ dominates life cycle $\mathbf{q}_2$ and write $\mathbf{q}_1 \geq_{\lambda_1} \mathbf{q}_2$. We also say that strategy $\mathbf{q}_i$ is optimal for given birth rates $\mathbf{b}$ and death rates $\mathbf{d}$ if it achieves the largest growth rate among all possible fragmentation modes, i.e., $\mathbf{q}_i \geq_{\lambda_1} \mathbf{q}_j$ for all $\mathbf{q}_j$ in the set of life cycles.

2.5 Two classes of fitness landscapes: fecundity landscapes and viability landscapes

Fitness landscapes capture the many advantages or disadvantages associated with group living. These advantages may come either in the form of additional resources available to groups depending on their size or as an improved protection from external hazards. For the sake of simplicity, we consider two classes of fitness landscape, each representing only one of these factors. In the first class, that we call "fecundity fitness landscapes", the group size affects only the birth rates of cells, while death rates remain independent of the group size; for convenience, we impose $d_i = 0$ for all i. In the second class, that we call "viability fitness landscapes", the group size affects only death rates, while birth

rates remain independent of the group size; in this case, we assume $b_i = 1$ for all i.

3 Results

3.1 Optimal life cycles are deterministic and characterised by binary fragmentation

We find that stochastic life cycles are dominated by a deterministic life cycle, i.e. for a given stochastic life cycle and fitness landscape it is always possible to find at least one deterministic life cycle that achieves a larger growth rate. As an illustration, consider the two deterministic strategies 1+1 and 2+1, and a stochastic strategy q mixing between these two deterministic modes so that with probability q fragmentation is governed by 2+1 and with probability $1-q$ it is governed by 1+1, i.e., a stochastic strategy represented by Eq. (2). For any mixing probability q and any fitness landscape $\{(b_1, b_2), (d_1, d_2)\}$, the growth rate λ_1^q of the corresponding stochastic strategy (given explicitly by Eq. (10)) is between the growth rates of the deterministic strategies, $\lambda_1^{1+1} \leq \lambda_1^q \leq \lambda_1^{2+1}$ or $\lambda_1^{2+1} \leq \lambda_1^q \leq \lambda_1^{1+1}$ holds. Hence, either the growth rate of 1+1 or the growth rate of 2+1 is larger than the growth rate of the stochastic strategy (Appendix A.2). Indeed, we are able to show a more general result: that for any fitness landscape and any maximum group size n, all stochastic strategies are dominated by at least one deterministic strategy. This allows us to conclude that the optimal life cycle is always a deterministic fragmentation mode (Appendix A.3).

We also find that, within the set of deterministic life cycles, "binary fragmentation" strategies (whereby groups split into exactly two offspring groups) dominate "non-binary fragmentation" strategies (whereby groups split into more than two offspring groups). To illustrate this result, consider the simplest case of $n = 3$ and the three deterministic strategies 1+1 (binary), 2+1 (binary), 1+1+1 (non-binary). By comparing the growth rates of the strategies, given by Eq. (13), we find that $\lambda_1^{1+1} \geq \lambda_1^{1+1+1}$ holds if $b_1 - b_2 \geq d_1 - d_2$ and that $\lambda_1^{2+1} \geq \lambda_1^{1+1+1}$ holds if $b_1 - b_2 \leq d_1 - d_2$. Thus, for any fitness landscape, 1+1+1 is dominated by either 2+1 or by 1+1. More generally, we can show that for any maximum group size n, any fitness landscape, and any non-binary fragmentation strategy, one can find a binary fragmentation strategy achieving a greater or equal growth rate (Appendix A.4). Hence, within the full space of strategies that we consider, only deterministic strategies characterised by binary fragmentation strategies are optimal.

Taken together, our analytical results imply that the set of optimal strategies is countable and, even

for large n, relatively small. As the number of strategies increases rapidly with n, we consider the proportion of deterministic strategies that can be optimal. While this is relatively high for small n (e.g., $2/3 \approx 0.67$ for $n = 3$ or $4/7 \approx 0.57$ for $n = 4$), it decreases sharply with increasing n (e.g., $25/128 \approx 0.20$ for $n = 10$ and $625/1295920 \approx 0.00048$ for $n = 50$).

Fig. 3 illustrates a numerical test of our findings for groups of maximum size $n = 4$ and a fecundity fitness landscape given by $\mathbf{b} = (1, b_2, 1.4)$ and $\mathbf{d} = (0, 0, 0)$. In line with our analysis, and for all values of b_2, the optimal life cycle is always characterised by deterministic binary fragmentation. In particular, for $b_2 = 2$, the optimal life cycle is 2+2, whereby groups grow up to size 4 and then immediately split into two bi-cellular groups (Fig. 3.*a*). Other deterministic binary fragmentation strategies can also be optimal, depending on the value of b_2 (Fig. 3.*b*). For small values ($b_2 \lesssim 0.45$), the production of bi-cellular complexes is too disadvantageous, hence the optimal life cycle is 1+1 (under which bi-cellular groups are not produced). For intermediary values ($0.45 \lesssim b_2 \lesssim 1.11$), the reproduction efficiency of three-cellular groups mitigates the inefficiency of two-cellular groups, and the strategy 3+1 becomes optimal. For larger values ($1.11 \lesssim b_2 \lesssim 3.52$), the optimal strategy is 2+2, where no independent cells are produced. Finally, for very large values ($b_2 \gtrsim 3.52$), the optimal strategy is 2+1, which ensures that one offspring group remains at the most productive bi-cellular state.

Fig. 4 shows the optimal life cycles for fecundity and viability landscapes and $n = 4$ (Appendix A.5). Under fecundity fitness landscapes where unicells have the largest birth rates, the optimal life cycle is 1+1. In this case, unicells perform better than larger cell complexes, and the optimal life cycle leads to populations consisting only of unicells. Under fitness landscapes where the birth rates of bi- and three-cellular complexes are similar and much larger than those of unicells, the optimal life cycle is 2+2. In this case, unicells perform worse than larger cell groups, and the optimal life cycle ensures that the population does not contain unicells. Under fitness landscapes where two cells have much higher birth rates than one cell or three cells, the optimal strategy is 2+1. In this case, the optimal life cycle keeps one of the offspring groups at the most productive state. The same argument holds for fitness landscapes where three cells have much higher birth rates than single cells or two cells, but in this case the optimal life cycle is 3+1. Under viability fitness landscapes, the performance of complexes improves with the decrease of the death rate. Thus, the map of optimal life cycles under viability landscapes follows the same qualitative pattern as under fecundity fitness landscapes.

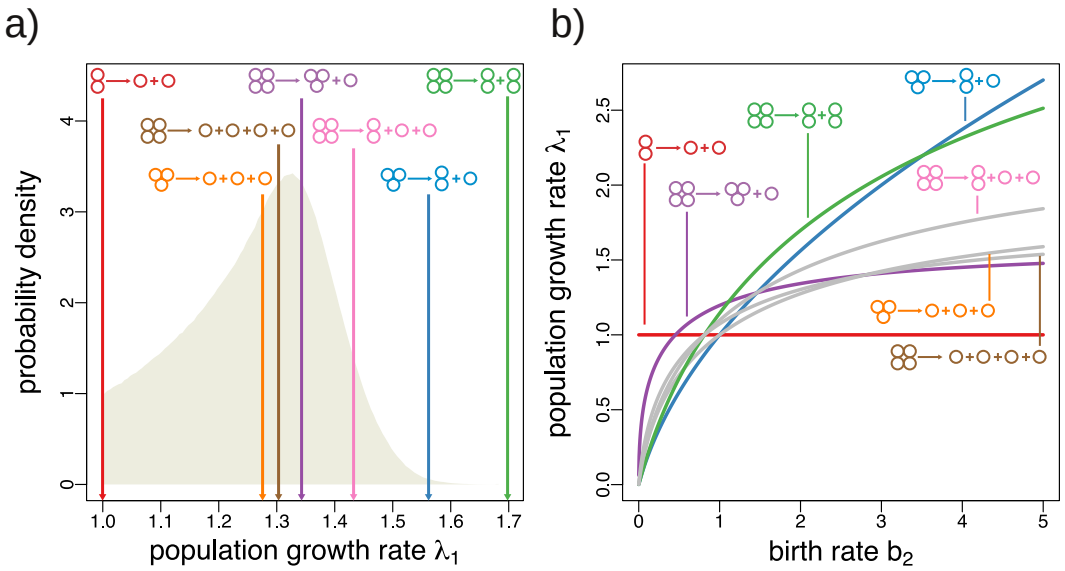

Figure 3: **Deterministic binary fragmentation is optimal.**

a) Empirical distribution of population growth rate of stochastic life cycles for $n = 4$ (generated from a sample of 10^7 randomly generated life cycles) subject to the fitness landscape $\{\mathbf{b}, \mathbf{d}\} = \{(1, 2, 1.4), (0, 0, 0)\}$. The population growth rates of all seven deterministic life cycles for $n = 4$ are indicated by arrows. Here, the deterministic life cycle 2+2 achieves the maximal possible growth rate among all possible life cycles. Random stochastic life cycles are generated as follows: The probabilities for growth without fragmentation are uniformly distributed. With the remaining probability, fragmentation occurs. The weight of each available fragmentation pattern is exponentially distributed.

b) Population growth rate (λ_1) for all seven deterministic life cycles for $n = 4$ subject to the fitness landscape $\{\mathbf{b}, \mathbf{d}\} = \{(1, b_2, 1.4), (0, 0, 0)\}$ as a function of the birth rate of bi-cells, b_2. Each of the four life cycles characterised by binary fragmentation (1+1, 2+1, 2+2, and 3+1) can be optimal depending on the value of b_2. Contrastingly, the three life cycles where a group fragments into more than two groups (1+1+1, 1+1+1+1, and 2+1+1) are never optimal.

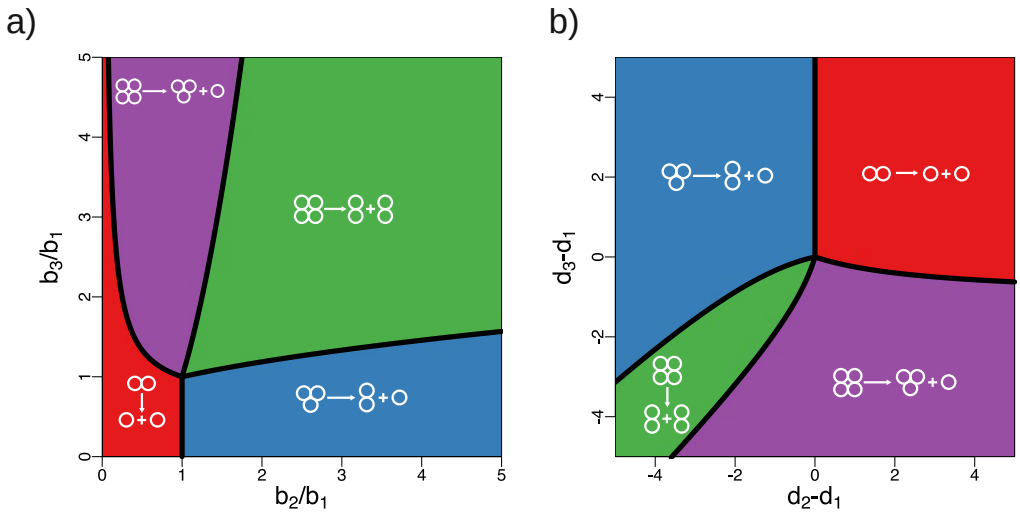

Figure 4: **Optimal life cycles for fecundity and viability fitness landscapes.** *(a)* Life cycles achieving the maximum population growth rate for $n = 4$ under fecundity fitness landscapes (i.e., $d_1 = d_2 = d_3 = 0$). In this scenario, the strategy 2+2 is optimal for most fitness landscapes. *(b)* Life cycles achieving the maximum population growth rate for $n = 4$ under viability fitness landscapes (i.e., $b_1 = b_2 = b_3 = 1$). In this scenario, life cycles emitting a unicellular propagule (1+1, 2+1, 3+1) are optimal for most parameter values. We use ratios of birth rates and differences between death rates as axes because one can consider $b_1 = 1$ and $\min(\mathbf{d}) = 0$ without loss of generality (Appendix A.1). Shaded areas are obtained from the direct comparison of the numerical solutions of characteristic equations in the form (11), lines are found analytically (Appendix A.5).

3.2 Synergistic interactions between cells promotes the production of unicelular propagules, while discounting interactions promote equal fragmentation.

Next, we focus on monotonic fitness landscapes for which either the birth rate of cells increases with group size (i.e., larger groups are more productive) or the death rate of groups decreases with group size (i.e., larger groups live longer). In particular, we consider fecundity fitness landscapes given by $b_i = 1 + Mg_i$ and $d_i = 0$ or viability fitness landscapes given by $b_i = 1$ and $d_i = M(1 - g_i)$, where $g_i = [(i-1)/(n-2)]^\alpha$ is the group size benefit [Fromhage and Kokko, 2011] and $M > 0$ is the maximum benefit. The parameter α is the degree of complementarity between different units (Fig. 5.*a*), it measures how important the addition of another unit is in producing the maximum possible benefit M [De Jaegher, 2017]. For $\alpha < 1$ the sequence g_i is strictly concave and the degree of complementarity is low: each additional unit in the group contributes less to the per capita benefit of group living [Hirshleifer, 1983], such that groups of all sizes achieve the same functionality as α tends to zero. For $\alpha = 1$ the sequence g_i is linear, and each additional unit contributes equally to the fitness of the group. Finally, for $\alpha > 1$, the sequence g_i is strictly convex and the degree of complementarity is high, with each additional unit improving the performance of the group more than the previous unit did. In the limit of large α, the advantages of group living materialise only when complexes achieve its maximum size $n - 1$ [Hirshleifer, 1983].

We numerically compute the optimal fragmentation modes for $n = 20$ and the fitness landscapes described above with $0.01 \leq \alpha \leq 100$ and $0.02 \leq M \leq 50$. We find that, for each value of α and M, the optimal life cycle is one where fragmentation occurs at the largest possible size (when the 20-th cell is born), i.e., a fragmentation mode belonging to the set $S = \{10 + 10, 11 + 9, \ldots, 19 + 1\}$. This is because the maximum of the benefit sequence g_i is at $i = 19$, so that groups of maximum size perform better, either by achieving the largest birth rate per unit (fecundity landscape) or the lowest death rate (viability landscape).

For low degrees of complementarity, the optimal life cycle is always to split into equally sized offspring groups. The intuition behind this result is that for very low complementarity, all multicellular groups ($i \geq 2$) have similar performance, while unicellular groups ($i = 1$) are at a significant disadvantage. Therefore, the optimal fragmentation mode is to ensure that both offspring groups are as large as possible, and hence of the same size. Contrastingly, for high degrees of complementarity, the optimal life cycle is always to fragment into one large group and one unicell. Here, the intuition is

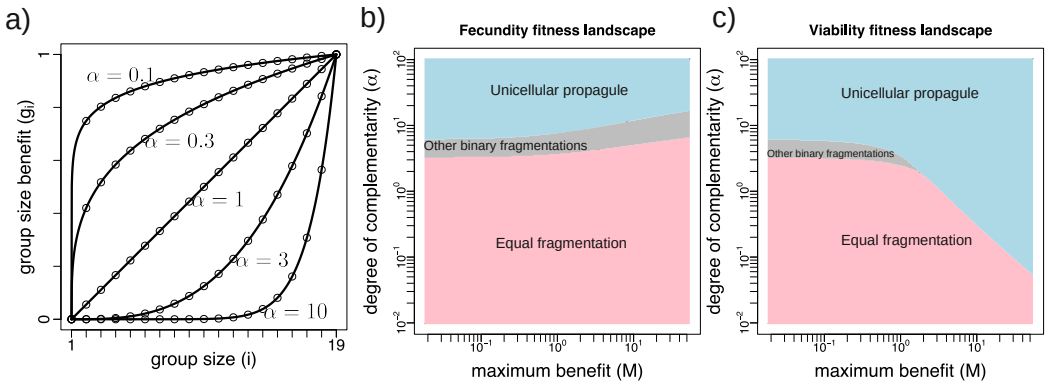

Figure 5: **"Equal fragmentation" and "unicellular propagule" fragmentation modes are often optimal under monotonic fitness landscapes.** *(a)* Group size benefit $g_i = [(i-1)/(n-2)]^\alpha$ as a function of group size for different values of the degree of complementarity α and $n = 20$. *(b)* Optimal life cycles under fecundity fitness landscapes with $b_i = 1 + Mg_i$ as a function of maximum benefit M and degree of complementarity α. Equal fragmentation is optimal if the degree of complementarity α is not too large. Increasing the maximum group size benefits M also promotes the evolution of equal fragmentation. *(c)* Optimal life cycles under viability fitness landscapes with $d_i = M(1 - g_i)$ as a function of M and α. Unicellular propagules are optimal if the degree of complementarity α is sufficiently large. An increase in the magnitude of group size bonus M also promotes the evolution of unicellular propagule.

that only the largest group can reap the benefits of group living and so the optimal mode is to have at least one offspring of very large size.

The optimal life cycle also depends on whether group size affects birth rate (fecundity landscapes) or death rate (viability landscapes). If a larger group size leads to an increase in the birth rate, then for low values of the maximum benefit M producing unicellular propagules is optimal only for high degrees of complementarity ($\alpha \gtrsim 7$). Larger values of M further rise the critical value of α above which the unicellular propagule is the optimal life cycle. Contrastingly, if a larger group size leads to a decrease in the death rate, then unicellular propagules can be optimal even if the degree of complementarity is low ($\alpha \lesssim 1$). In general, benefits on the birth rate make equal fragmentation optimal under more demographic scenarios. On the contrary, benefits on the death rate make unicellular propagule optimal under more demographic scenarios.

3.3 Costly fragmentation allows splitting into multiple offspring groups to be optimal

Up to this point, we have assumed that fragmentation is costless. However, fragmentation processes can be costly to the parental group undergoing division. Reproduction costs are apparent in the case of *Volvox*, where somatic cells constituting the outer layer of the group die upon releasing the offspring cells and are not passed to the next generation [Kirk, 2005]. Reproduction costs may also be less apparent. For instance, group division may cost resources that would otherwise be available for the growth of cells within a group.

To investigate the effect of fragmentation costs on the set of optimal life cycles, we assume that exactly one cell is lost upon each fragmentation event, so that the total number of cells in offspring groups is one less than the number of cells in the parental group. Mathematically, this implies that, upon reaching size $i+1$, fragmentation patterns are described by partitions of i rather than by partitions of $i+1$ (Appendix A.6).

For such kind of costly fragmentation, stochastic life cycles are still dominated by deterministic life cycles (a proof similar to the one given in Appendix A.3 for costless fragmentation still holds in this case). However, under costly fragmentation, the set of optimal life cycles can also comprise instances of non-binary fragmentation (i.e., division into more than two offspring groups). This can be readily illustrated for the case of $n = 4$ where the mode 1+1+1 is optimal for a wide range of fitness landscapes (Fig. 6).

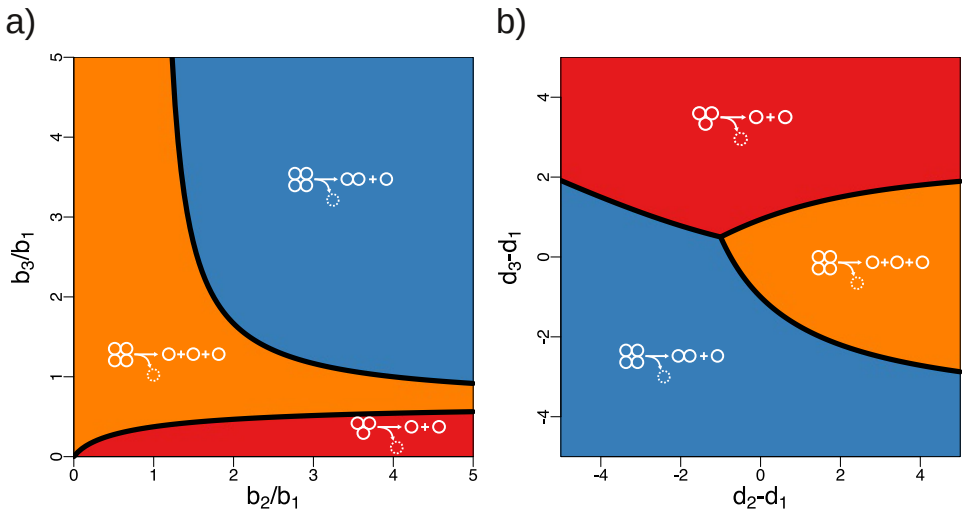

Figure 6: **Optimal life cycles for fecundity and viability fitness landscapes under costly fragmentation.** Under costly fragmentation, each splitting event is associated with the loss of one cell. *(a)* Life cycles achieving the maximum population growth rate for $n = 4$ under fecundity fitness landscapes (i.e., $d_1 = d_2 = d_3 = 0$). *(b)* Life cycle strategies achieving the maximum population growth rate for $n = 4$ under viability fitness landscapes (i.e., $b_1 = b_2 = b_3 = 1$). In both classes of fitness landscapes, the life cycle 1+1+1, whereby 4-unit complexes produce 3 surviving independent units, is optimal under a wide range of fitness landscapes.

Another notable effect provided by the scenario of costly fragmentation is that life cycles involving the emergence of large groups may be optimal even if groups do not grant any advantage to cells. If fragmentation is costless, as we assumed above, fitness landscapes for which groups have inferior performance in comparison with independent cells (that is, $b_i/b_1 \leq 1$ for fecundity landscapes or $d_i - d_1 \geq 0$ for viability landscapes) lead to optimal life cycles where fragmentation occurs at the minimal possible group size $i = 2$, so that no multicellular groups emerge in the population (see Fig. 4). Contrastingly, in the case of costly fragmentation some of these fitness landscapes promote fragmentation modes in which groups split at the maximal available size $n = 4$. Thus, the population may contain multi-celled groups, even if these groups perform strictly worse than independent cells. Such a counterintuitive behavior can be evolutionarily optimal, because the burden of inevitable cell loss is indirectly shared among multiple offspring groups. Thus, the growth to a large size and then fragmentation into multiple offspring groups minimizes the cost of cell loss and might be therefore beneficial, even if the groups themselves are at a disadvantage.

We also identified optimal life cycles under costly fragmentation for larger group sizes and monotonic fitness landscapes (Fig. 7). To obtain results comparable to the case of costless fragmentation, we increased the group size limit by one, i.e., we assumed $n = 21$, so that the sum of offspring sizes in both cases is equal to 20. Similarly to the case of costless fragmentation, all optimal life cycles are such that splitting occurs only at the maximal possible size n. However, under costly fragmentation, a new class of life cycle may be optimal: splitting into more than two offspring groups of similar size; we call a life cycle within this class a "multiple fragmentation mode". The most prominent mode in this class is the fragmentation into multiple independent cells, i.e., 1+1+...+1. This fragmentation mode is promoted by fitness landscapes with low maximum benefit ($M < 1$). Under these fitness landscapes, the group size has a small impact on the group performance, so the fragmentation cost becomes the main factor determining the optimality of life cycles. The optimal mode to minimize the fragmentation cost is to produce the maximal number of offspring per fragmentation event, i.e., to fragment into independent cells.

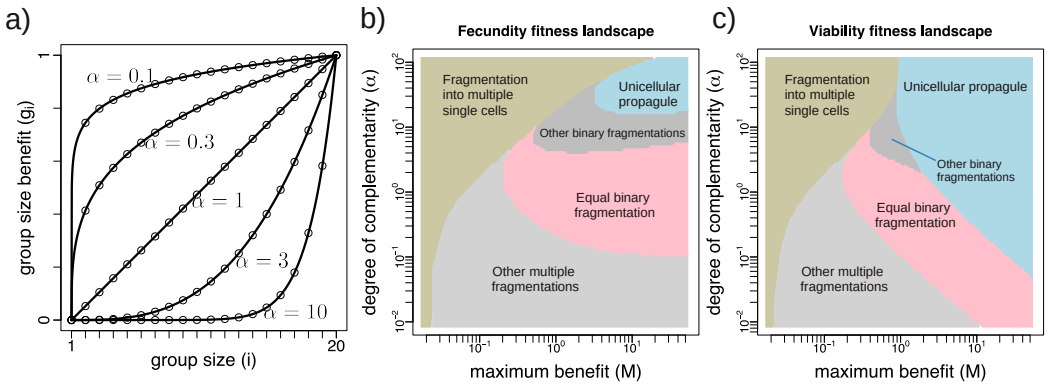

Figure 7: **Multiple fragmentation into groups of similar size can be optimal under costly fragmentation and monotonic fitness landscapes.** *(a)* Group size benefit $g_i = [(i-1)/(n-2)]^{\alpha}$ as a function of group size for different values of the degree of complementarity α and $n = 21$. *(b)* Optimal life cycles under fecundity fitness landscapes with $b_i = 1 + Mg_i$ as a function of maximum benefit M and degree of complementarity α. The fragmentation into multiple single cells is described by the fragmentation pattern 1+1+...+1; other multiple fragmentation strategies have patterns 2+2+...+2, 3+3+3+3+3+3+2, 4+4+3+3+3+3, 4+4+4+4+4, 5+5+5+5, and 7+7+6. They are all coloured together as a single light gray area. *(c)* Optimal life cycles under viability fitness landscapes with $d_i = M(1-g_i)$ as a function of M and α.

4 Discussion

Reproduction is such a fundamental feature of living systems that the idea that the mode of reproduction may be shaped by natural selection is easily overlooked. Here, we analysed a matrix population model that captures the demographic dynamics of complexes that grow by staying together and reproduce by fragmentation. The costs and benefits associated with group size determine whether or not a single cell fragments into two separate daughter cells upon cell division, or whether those daughter cells remain in close proximity, with fragmentation occurring only after subsequent rounds of division.

We showed that for each stochastic fragmentation mode there is a deterministic fragmentation mode that leads to higher cellular growth rate. Such a deterministic mode involves a regular schedule of group development and fragmentation. We also showed that, for any fitness landscape where fragmentation occurs without cell loss, the optimal fragmentation mode always involves binary fragmentation. It is important to note that this does not mean that, for a given fitness landscape, a given mode with binary fragmentation will necessarily outperform a non-binary fragmentation mode. Instead, for any given fitness landscape the best possible mode of reproduction will be one that involves

binary fragmentation. For example, with reference to Fig. 3*b* and for low b_2, a group of three cells that fragments into 1+1+1 outperforms three cells that undergo binary fragmentation producing 2+1. However, 1+1+1 is outperformed by the unicellular life cycle 1+1, and also by groups of four cells that fragment into 3+1.

A particularly intriguing finding is that the optimal life cycle under monotonic fitness landscapes is generally of one of two types: "equal fragmentation", which involves fission into two equal size groups, and "unicellular propagule", which involves the production of two groups, one comprised of a single cell (Fig. 5). Equal fragmentation is favoured when there is a significant advantage associated with formation of even the smallest group, whereas unicellular propagule is favoured when the benefits associated with group size are not evident until groups become large. This makes intuitive sense: when advantages arise when groups are small, it pays for offspring to be groups (and not single cells). Conversely, when there is little gain until group size is large, it makes sense to maintain one group that reaps this advantage.

Many multicellular organisms are characterised by a life cycle in which adult individuals develop from a single cell [Grosberg and Strathmann, 1998]. Although passing through a unicellular bottleneck is a requirement for sexual reproduction, life cycles with unicellular stages are also common in asexual organisms such as multicellular algae and ciliates [Herron et al., 2013]. If multicellularity evolved because of the benefits associated to group living, why do so many multicellular organisms begin their life cycles as solitary (and potentially vulnerable) cells? Explanatory hypotheses include the purge of deleterious mutations and the reduction of within-organism evolutionary conflict resulting from clonality [Maynard Smith and Szathmáry, 1995, Grosberg and Strathmann, 1998]. Our results make the case for an alternative (and perhaps more parsimonious) answer to this question: for relatively high degree of complementarity on the number of cells of an organism, a life cycle featuring a unicellular bottleneck is just the best way to guarantee that the "parent" group remains as large as possible to reap off the maximum fecundity and/or viability advantages of group living. Our theoretical results resonate with previous experimental work demonstrating that single-cell bottlenecks can be adaptive simply because they maximise growth rate [Ratcliff et al., 2013].

Once cell loss upon fragmentation is incorporated as a factor in collective reproduction, a wider range of fragmentation patterns become optimal. Such optimal life cycles include those where splitting involves the production of multiple offspring (including multiple independent cells). These strategies

are optimal under conditions where there is negligible benefit associated with group size (Fig. 7). Intuitively, this is because the production of multiple offspring allows the cost of cell loss to be spread among many offspring.

This distribution of costs among offspring may also explain the tendency for life cycles involving larger groups to outperform life cycles that fragment at smaller group size under fitness landscapes that penalize groups of increasing size (e.g., when $b_1 > b_2 > b_3$). In the absence of a cost due to cell loss, such landscapes favour the unicellular life cycle (Fig. 4a). With costs associated with cell loss, not only is the unicellular life cycle excluded, but life cycles involving large groups can be favoured over those involving smaller groups. This is evident in Fig. 6: under the fitness landscape given by $\{\mathbf{b}, \mathbf{d}\} = \{(1, 0.9, 0.8), (0, 0, 0)\}$, groups that fragment at four cells outperform groups that fragment at three cells. This reflects the fact that groups growing up to four cells before fragmentation distribute the cost of cell loss among the three remaining cells, whereas a group that reaches three cells before fragmentation distributes the cost among just two offspring cells.

Previous theoretical work has explored several questions related to the evolution of multicellularity using matrix population models similar to the one proposed in this paper. In a seminal contribution, Roze and Michod [2001] explored the evolution of propagule size in the face of deleterious and selfish mutations. In their model, multicellular groups first grow up to an adult size and then reproduce by splitting into equally sized groups, so that life cycle strategies can be indexed by the size of the propagule size. In our terminology, this refers to the class of (deterministic) "multiple fragmentation modes". An important finding of Roze and Michod [2001] is that, even if large groups are advantageous, small propagules can be often selected because they are more efficient at eliminating detrimental mutations. Contrastingly, we did not study the effects of mutations, as cells in our model replicate faithfully. Instead, we allowed for general fitness landscapes and the whole space of fragmentation modes, including cases of asymmetric binary division (e.g. the "unicellular propagule" strategy) neglected by Roze and Michod [2001]. Our results indicate that reproduction modes involving unicells often lead to the maximum growth rate even when large group sizes confer fecundity or viability advantages making small propagule sizes to either divide less efficiently or die at a higher rate. In particular, we have shown that if fragmentation is costly, a strategy consisting of a multiple fragmentation mode with propagule size one (i.e., the small propagule strategy studied by Roze and Michod [2001]) can be adaptive for reasons different than the elimination of harmful mutations. Extending our model to

allow for mutations giving rise to heterogenous collectives characterised by within-organism conflict or division of labor is a possible avenue of future research that would complement recent theoretical efforts [Rashidi et al., 2015, Kaveh et al., 2016].

Closer to our work, Tarnita et al. [2013] investigated the evolution of multicellular life cycles via two alternative routes: "staying together" (whereby offspring cells remain attached to the parent) and "coming together" (whereby cells of different origins aggregate in a group). In particular, they studied the conditions under which a multicellular strategy that grow complexes via staying together can outperform a solitary strategy whereby cells always separate after division. The way they model group formation and analyze the resulting population dynamics (by means of biological reactions and matrix models) is closely related to our approach; indeed, their solitary strategy is our binary strategy 1+1, while their staying together strategy corresponds to a particular kind of binary stochastic strategy. The questions we ask are however different. Tarnita et al. [2013] were concerned with the conditions under which (multicellular) strategies that form groups can invade and replace (unicellular) strategies that remain solitary; to do so they postulated specific reproductive modes and allowed for multicellular and unicellular strategies to experience different birth and death rates (fitness landscapes). Contrastingly, we aimed to understand what would be, for a common fitness landscape, the optimal reproduction mode out of the vast space of fragmentation strategies comprising all possible deterministic and probabilistic pathways by which complexes stay together and split apart. A key finding is that for any fitness landscape, stochastic modes of fragmentation such as the particular staying together strategy considered by Tarnita et al. [2013], will be outperformed by at least one deterministic fragmentation mode. With all the apparent generality of probabilistic reproduction modes, our model predicts that life cycles shaped by natural selection will be characterised by a highly regulated developmental program.

Other than diagnostic value, modes of fragmentation in bacteria have received little attention. The theoretical framework developed here could serve as a null hypothesis against which the adaptive significance of modes of fragmentation can be examined. It is of interest to note that two bacteria that form groups and are well studied from a clinical perspective, *Neisseria gonorrhoeae* and *Staphylococcus aureus*, both show evidence of deterministic fragmentation by binary fragmentation: *Neisseria gonorrhoeae* divide into groups of two equal sizes [Westling-Häggström et al., 1977]. *Staphylococcus aureus* divide into one large group plus a unicellular propagule [Koyama et al., 1977]. This leads to

411 questions concerning the nature of the fitness landscape occupied by these bacteria and the basis of
412 any collective level benefit as assumed by our model.

413 Although cell loss (apoptosis) is known in bacteria [Rice and Bayles, 2008], it is not usually, with
414 the exception of cyanobateria [Rossetti et al., 2011], associated with fragmentation. However, cell loss
415 upon fragmentation occurs in *Volvox carteri*, a member of the volvacine algae, where the outer (soma)
416 cells, while contributing to collective viability, undergo senescence and die following the liberation of
417 the germ line cells [Kochert, 1968, Kirk, 2005]. In our model, such a mode of reproduction is possible
418 in instances where cell loss is associated with fragmentation. Within the volvacine algae, there are
419 species, such as *Gonium pectorale*, that also fragment into multiple propagules in the absence of cell
420 death. Although costs associated with cell loss are not evident, it is nonetheless likely that the process
421 of fragmentation is costly, for example, arising from production of enzymes for the degradation of the
422 cell matrix [Birkendal-Hansen, 1995, Basbaum and Zena, 1996].

423 While the model developed here is conceptually simple, it is readily extended and applied to the
424 study of more complex life cycles, including those involving specialized cell types, such as germ and
425 soma cells as found in many multicellular organisms. Our model is also amenable to exploring the
426 effects of developmental structure on the selective benefit of differing modes of reproduction.

427 5 Acknowledgements

428 Our work was supported by DAAD Short-Term Research Grant #57130097 (to Y.P.)

429 References

430 G.E. Andrews. *The Theory of Partitions*. Cambridge University Press, Cambridge, UK, 1998.

431 E.R. Angert. Alternatives to binary fission in bacteria. *Nature Reviews Microbiology*, 3(3):214–224,
432 2005.

433 C.B. Basbaum and W. Zena. Focalized proteolysis: spatial and temporal regulation of extracellular
434 matrix degradation at the cell surface. *Current Opinion in Cell Biology*, 8(5):731 – 738, 1996.

435 H. Birkendal-Hansen. Proteolytic remodeling of extracellular matrix. *Current Opinion in Cell Biology*,
436 7(5):728 – 735, 1995.

437 J.T. Bonner. Evolutionary strategies and developmental constraints in the cellular slime molds. *The*
438 *American Naturalist*, 119(4):530 – 552, 1982.

439 M. E. Boraas, D. B. Seale, and J. E. Boxhorn. Phagotrophy by a flagellate selects for colonial prey: A
440 possible origin of multicellularity. *Evolutionary Ecology*, 12(2):153–164, 1998.

441 S. Boyd and L. Vandenberghe. *Convex Optimization*. Cambridge university press, 2004.

442 H. Caswell. *Matrix Population Models*. Sinauer Associates, 2nd edition edition, 2001.

443 J. E. Cohen. Convexity of the dominant eigenvalue of an essentially nonnegative matrix. *Proceedings*
444 *of the American Mathematical Society*, 81(4):657–658, 1981.

445 K. De Jaegher. Harsh environments and the evolution of multi-player cooperation. *Theoretical Popu-*
446 *lation Biology*, 113:1 – 12, 2017.

447 C. de la Fuente-Núñez, F. Reffuveille, L. Fernández, and R. E. W. Hancock. Bacterial biofilm devel-
448 opment as a multicellular adaptation: antibiotic resistance and new therapeutic strategies. *Current*
449 *Opinion in Microbiology*, 16(5):580 – 589, 2013.

450 S.P. Diggle, A.S. Griffin, G.S. Campbell, and S.A. West. Cooperation and conflict in quorum-sensing
451 bacterial populations. *Nature*, 450(7168):411–414, 2007.

452 L. Fromhage and H. Kokko. Monogamy and haplodiploidy act in synergy to promote the evolution of
453 eusociality. *Nature Communications*, 2:397, 2011.

454 P. Godfrey-Smith. *Darwinian Populations and Natural Selection*. Oxford University Press, 2009.

455 K. Groebe and W. Mueller-Klieser. On the relation between size of necrosis and diameter of tumor
456 spheroids. *International Journal of Radiation Oncology*Biology*Physics*, 34(2):395 – 401, 1996.

457 R. K. Grosberg and R. R. Strathmann. One cell, two cell, red cell, blue cell: the persistence of a
458 unicellular stage in multicellular life histories. *Trends in Ecology & Evolution*, 13(3):112 – 116,
459 1998.

460 K. Hammerschmidt, C. J. Rose, B. Kerr, and P. B. Rainey. Life cycles, fitness decoupling and the
461 evolution of multicellularity. *Nature*, 515(7525):75–79, 2014.

M.D. Herron, A. Rashidi, D. E. Shelton, and W. W. Driscoll. Cellular differentiation and individuality in the 'minor' multicellular taxa. *Biological Reviews*, 88(4):844–861, 2013. ISSN 1469-185X. doi: 10.1111/brv.12031. URL `http://dx.doi.org/10.1111/brv.12031`.

J. Hirshleifer. From weakest-link to best-shot: The voluntary provision of public goods. *Public Choice*, 41(3):371–386, 1983.

K. Kaveh, C. Veller, and M. A. Nowak. Games of multicellularity. *Journal of Theoretical Biology*, 403:143 – 158, 2016.

D. L. Kirk. A twelve step program for evolving multicellularity and a division of labor. *BioEssays*, 27 (3):299–310, 2005.

G. Kochert. Differentiation of reproductive cells in volvox carteri. *The Journal of Protozoology*, 15 (3):438 – 452, 1968.

T. Koyama, M. Yamada, and M. Matsuhashi. Formation of regular packets of staphylococcus aureus cells. *Journal of Bacteriology*, 129(3):1518 – 1523, 1977.

E. Libby and P. B. Rainey. A conceptual framework for the evolutionary origins of multicellularity. *Physical Biology*, 10(3):035002, 2013.

J. Maynard Smith and E. Szathmáry. *The Major Transitions in Evolution*. W. H. Freeman, Oxford, 1995.

P. B. Rainey and S. De Monte. Resolving conflicts during the evolutionary transition to multicellular life. *Annual Review of Ecology, Evolution, and Systematics*, 45:599 – 620, 2014.

A. Rashidi, D. E. Shelton, and R. E. Michod. A darwinian approach to the origin of life cycles with group properties. *Theoretical Population Biology*, 102:76 – 84, 2015.

W. C. Ratcliff, M. D. Herron, K. Howell, J. T. Pentz, F. Rosenzweig, and M. Travisano. Experimental evolution of an altering uni- and multicellular life cycle in chlamydomonas reinhardtii. *Nature Communications*, 4(2742), November 2013.

K.C. Rice and K.W. Bayles. Molecular control of bacterial death and lysis. *Microbiology and Molecular Biology Reviews*, 72(1):85 – 109, 2008.

V. Rossetti, M. Filippini, M. Svercel, A. D. Barbour, and H. C. Bagheri. Emergent multicellular life cycles in filamentous bacteria owing to density-dependent population dynamics. *Journal of The Royal Society Interface*, 8(65):1772–1784, 2011. doi: 10.1098/rsif.2011.0102.

D. Roze and R. E. Michod. Mutation, multilevel selection, and the evolution of propagule size during the origin of multicellularity. *The American Naturalist*, 158(6):638 – 654, 2001.

P. S. Stewart and M. J. Franklin. Physiological heterogeneity in biofilms. *Nature Reviews Microbiology*, 6(3):199 – 210, 2008.

C. E. Tarnita, C. H. Taubes, and M. A. Nowak. Evolutionary construction by staying together and coming together. *Journal of Theoretical Biology*, 320(0):10–22, 2013.

B. Westling-Häggström, T.H. Elmros, S.T. Normark, and B. Winblad. Growth pattern and cell division in neisseria gonorrhoeae. *Journal of Bacteriology*, 129(1):333–342, 1977.

P. Williams, N. J. Bainton, S. Swift, S. R. Chhabra, M. K. Winson, G. S. Stewart, GPC Salmond, and B. W. Bycroft. Small molecule-mediated density-dependent control of gene expression in prokaryotes: bioluminescence and the biosynthesis of carbapenem antibiotics. *FEMS Microbiology Letters*, 100(1-3):161 – 167, 1992.

A Appendix

A.1 Characteristic equation of a deterministic fragmentation mode

Consider a deterministic fragmentation mode in which a group of size m grows to size $m+1$ and fragments according to fragmentation pattern $\kappa \vdash m+1$. The corresponding projection matrix is an $m \times m$ matrix of the form

$$\mathbf{A} = \begin{pmatrix} -b_1 - d_1 & 0 & \cdots & 0 & mb_m\pi_1(\kappa) \\ b_1 & -2b_2 - d_2 & 0 & \vdots & mb_m\pi_2(\kappa) \\ 0 & 2b_2 & -3b_3 - d_3 & 0 & mb_m\pi_3(\kappa) \\ 0 & 0 & \ddots & \ddots & \vdots \\ 0 & 0 & \cdots & (m-1)b_{m-1} & mb_m\pi_m(\kappa) - mb_m - d_m \end{pmatrix}.$$

The population growth rate is given by the leading eigenvalue λ_1 of $\mathbf{A}$, i.e., the largest solution of the characteristic equation

$$\det\left(\mathbf{A}-\lambda\mathbf{I}\right)=0. \tag{14}$$

By using a Laplace expansion along the last column of $\mathbf{A}-\lambda\mathbf{I}$, we can rewrite the left hand side of the above expression (i.e., the characteristic polynomial of $\mathbf{A}$) as

$$\begin{aligned}\det\left(\mathbf{A}-\lambda\mathbf{I}\right) &= \sum_{i=1}^{m-1}(-1)^{i+m}mb_m\pi_i(\kappa)M_{i,m}+(-1)^{2m}\left(mb_m\pi_m(\kappa)-mb_m-d_m-\lambda\right)M_{m,m}\\ &= \sum_{i=1}^{m}(-1)^{i+m}mb_m\pi_i(\kappa)M_{i,m}-\left(mb_m+d_m+\lambda\right)M_{m,m}\end{aligned} \tag{15}$$

where $M_{i,m}$ is the (i,m) minor of $\mathbf{A}-\lambda\mathbf{I}$. For all $i=1,\ldots,m$, the minor $M_{i,m}$ is the determinant of a block diagonal matrix, and hence equal to the product of the determinants of the diagonal blocks. Moreover, each diagonal block is either a lower triangular or an upper triangular matrix, whose determinant is given by the product of the elements in their main diagonals. We can then write

$$M_{i,m}=\prod_{j=1}^{i-1}\left(-jb_j-d_j-\lambda\right)\prod_{j=i}^{m-1}jb_j. \tag{16}$$

Substituting Eq. (16) into Eq. (15) and simplifying, we obtain

$$\begin{aligned}\det\left(\mathbf{A}-\lambda\mathbf{I}\right) &= (-1)^{m-1}\sum_{i=1}^{m}mb_m\pi_i(\kappa)\prod_{j=1}^{i-1}\left(jb_j+d_j+\lambda\right)\prod_{j=i}^{m-1}jb_j\\ &\quad-(-1)^{m-1}\left(mb_m+d_m+\lambda\right)\prod_{j=1}^{m-1}\left(jb_j+d_j+\lambda\right)\\ &= (-1)^{m-1}\left[\prod_{j=1}^{m}jb_j\right]\left(\left[\sum_{i=1}^{m}\pi_i(\kappa)\prod_{j=1}^{i-1}\left(1+\frac{d_j+\lambda}{jb_j}\right)\right]-\prod_{j=1}^{m}\left(1+\frac{d_j+\lambda}{jb_j}\right)\right).\end{aligned}$$

Replacing this expression into the characteristic equation (14), dividing both sides by $(-1)^m\prod_{j=1}^{m}jb_j$, and simplifying, we finally obtain that the characteristic equation (14) can be written as

$$F_{m+1}(\lambda)-\sum_{i=1}^{m}\pi_i(\kappa)F_i(\lambda)=0, \tag{17}$$

where

$$F_i(\lambda)=\prod_{j=1}^{i-1}\left(1+\frac{d_j+\lambda}{jb_j}\right). \tag{18}$$

Note that two transformations preserve the solution of Eq. (17)

$$\mathbf{d}\to\mathbf{d}-r,\qquad\lambda\to\lambda+r,\qquad r\leq\min(\mathbf{d}),$$

and

$$\mathbf{d} \to s\mathbf{d}, \qquad \mathbf{b} \to s\mathbf{b}, \qquad \lambda \to s\lambda, \qquad s > 0.$$

These transformations allow us to set $b_1 = 1$ and $\min(\mathbf{d}) = 0$ without loss of generality.

A.2 Mixing between 1+1 and 2+1 is dominated

To show that the life cycle mixing between fragmentation modes 1+1 and 2+1 with probability q and represented by Eq. (2) is dominated, consider its growth rate λ_1^q as a function of q, as given by Eq. (10). We have $\lambda_1^q(0) = \lambda_1^{1+1}$ and $\lambda_1^q(1) = \lambda_1^{2+1}$. A sufficient condition for q to be dominated by either 1+1 or 2+1 is then that $\lambda_1^q(q)$ is monotonic in q. To show that this is the case, note that the derivative of λ_1^q with respect to q is given by

$$\frac{d\lambda_1^q}{dq} = b_1 \left(-1 + \frac{(2q-1)b_1 + 2b_2 + d_1 - d_2}{\sqrt{((2q-1)b_1 + d_1 + d_2)^2 + 4b_1(2qb_2 - (2q-1)d_2) - 4d_1 d_2}} \right),$$

and that such expression is equal to zero if and only if

$$b_1 - b_2 = d_1 - d_2 \tag{19}$$

which is independent of q. It follows that λ_1^q is either nonincreasing or nondecreasing in q, and hence that it attains its maximum at either $q = 0$, $q = 1$, or (when (19) is satisfied) at any $q \in [0, 1]$. Hence, q is dominated by either 1+1 or 2+1.

A.3 Stochastic fragmentation modes are dominated

For any fitness landscapes, stochastic fragmentation modes are dominated by at least one deterministic mode. In other words, the optimal life cycle is deterministic. To prove this, consider the set of partitions $\kappa \vdash j$ for a given j, fix the probabilities of fragmentation patterns $\nu \vdash i \neq j$ to arbitrary values, and focus attention on the function

$$\lambda_1^j : S_j \to \mathbb{R},$$

mapping probability distributions in the ζ_j-simplex $S_j \subset \mathbb{R}^{\zeta_j}$ (specifying the probabilities of all partitions $\kappa \vdash j$) to the dominant eigenvalue λ_1^j of the associated projection matrix $\mathbf{A}$. Our goal is to show that, for any j, λ_1^j is a quasiconvex function, i.e., that

$$\lambda_1^j(\eta\mathbf{x}_1 + (1-\eta)\mathbf{x}_2) \leq \max\left\{\lambda_1^j(\mathbf{x}_1), \lambda_1^j(\mathbf{x}_2)\right\}$$

holds for all $\mathbf{x}_1, \mathbf{x}_2 \in S_j$ and $\eta \in [0,1]$. Quasiconvexity of λ_1^j implies that λ_1^j achieves its maximum at an extreme point of S_j, i.e., at a probability distribution that puts all of its mass in a single fragmentation pattern. Quasiconvexity of λ_1^j for all j then implies that the maximum growth rate λ_1 is achieved by a deterministic fragmentation mode, and that stochastic fragmentation modes are dominated.

To show that λ_1^j is quasiconvex, we restrict the function to an arbitrary line and check quasiconvexity of the resulting scalar function [Boyd and Vandenberghe, 2004, p. 99]. More precisely, we aim to show that the function

$$\ell(t) = \lambda_1^j \left(\mathbf{u} + t\mathbf{v}\right),$$

is quasiconvex in t for any $\mathbf{u} \in S_j$ and $\mathbf{v} \in \mathbb{R}^{\zeta_j}$ such that $\mathbf{u} + t\mathbf{v} \in S_j$. We hence need to verify that

$$\ell(\tau t_1 + (1-\tau)t_2) \leq \max\left\{\ell(t_1), \ell(t_2)\right\} \tag{20}$$

holds for $\tau \in [0,1]$.

To show this, note that the function $\ell(t) = \lambda_1^j(\mathbf{u} + t\mathbf{v})$ is given implicitly as the largest root of the characteristic polynomial

$$p(\lambda) = \det\left(\mathbf{A} - \lambda\mathbf{I}\right), \tag{21}$$

where the probabilities of fragmentation specified by $\mathbf{u} + t\mathbf{v}$ appear in the $(j-1)$-th column of the projection matrix $\mathbf{A}$ (see Eq. (8)).

The right hand side of Eq. (21) can be written using a Laplace expansion along the $(j-1)$-th column of $\mathbf{A} - \lambda\mathbf{I}$, i.e.,

$$\det(\mathbf{A} - \lambda\mathbf{I}) = \sum_{i=0}^{n-1} (-1)^{i+j-1} (a_{i,j-1} - \delta_{i,j-1}\lambda) M_{i,j-1}, \tag{22}$$

where $\delta_{i,j-1}$ is the Kronecker delta and $M_{i,j-1}$ is the $(i, j-1)$ minor of $\mathbf{A}$, i.e., the determinant of the submatrix obtained from $\mathbf{A}$ by deleting the i-th row and $(j-1)$-th column. Each minor $M_{i,j-1}$ is independent of t because the only entries of $\mathbf{A}$ that depend on t appear in the $(j-1)$-th column. Moreover, each entry $a_{i,j-1}$ is either zero or a linear function of t. Hence, $p(\lambda)$ is a polynomial on λ with coefficients that are linear in t, i.e., of the form

$$p(\lambda) = \sum_{k=0}^{n-1} \left(\alpha_k + \beta_k t\right) \lambda^k, \tag{23}$$

for some α_k, β_k. Moreover, since the leading coefficient must be $(-1)^{n-1}$ (the matrix $\mathbf{A}$ is $(n-1) \times (n-1)$), it follows that $\alpha_{n-1} = (-1)^{n-1}$ and $\beta_{n-1} = 0$.

Denote by $p_\tau(\lambda)$, $p_1(\lambda)$, and $p_2(\lambda)$ the characteristic polynomials corresponding to, respectively, the probability distributions given by $\mathbf{u} + [\tau t_1 + (1-\tau)t_2]\,\mathbf{v}$, $\mathbf{u} + t_1\mathbf{v}$, and $\mathbf{u} + t_2\mathbf{v}$. From Eq. (23), these are given by

$$p_\tau(\lambda) = \sum_{k=0}^{n-1} \left(\alpha_k + \beta_k \left[\tau t_1 + (1-\tau)t_2\right]\right) \lambda^k = \sum_{k=0}^{n-1} \alpha_k \lambda^k + \left[\tau t_1 + (1-\tau)t_2\right] \sum_{k=0}^{n-1} \beta_k \lambda^k \tag{24a}$$

$$p_1(\lambda) = \sum_{k=0}^{n-1} \left(\alpha_k + \beta_k t_1\right) \lambda^k = \sum_{k=0}^{n-1} \alpha_k \lambda^k + t_1 \sum_{k=0}^{n-1} \beta_k \lambda^k \tag{24b}$$

$$p_2(\lambda) = \sum_{k=0}^{n-1} \left(\alpha_k + \beta_k t_2\right) \lambda^k = \sum_{k=0}^{n-1} \alpha_k \lambda^k + t_2 \sum_{k=0}^{n-1} \beta_k \lambda^k \tag{24c}$$

Subtracting Eq. (24b) from Eq. (24a), and Eq. (24c) from Eq. (24a), we can write

$$p_\tau(\lambda) - p_1(\lambda) = (t_2 - t_1)(1-\tau) \sum_{k=0}^{n-1} \beta_k \lambda^k,$$

$$p_\tau(\lambda) - p_2(\lambda) = (t_1 - t_2)\tau \sum_{k=0}^{n-1} \beta_k \lambda^k.$$

Note that the signs of these differences are always different, i.e., either (i) $p_\tau(\lambda) - p_1(\lambda) \geq 0$ and $p_\tau(\lambda) - p_2(\lambda) \leq 0$, or (ii) $p_\tau(\lambda) - p_1(\lambda) \leq 0$ and $p_\tau(\lambda) - p_2(\lambda) \geq 0$. In the first case, we have $p_1(\lambda) \leq p_\tau(\lambda) \leq p_2(\lambda)$ and in the second we have $p_2(\lambda) \leq p_\tau(\lambda) \leq p_1(\lambda)$, i.e., for each λ, $p_\tau(\lambda)$ lies between $p_1(\lambda)$ and $p_2(\lambda)$, or, equivalently

$$p_\tau(\lambda) \leq \max\left\{p_1(\lambda), p_2(\lambda)\right\}, \tag{25}$$

for all λ. Since λ_1^j is the largest root of $p(\lambda)$, and since $p_\tau(\lambda)$, $p_1(\lambda)$, and $p_2(\lambda)$ all have the same sign in the limit when λ tends to infinity (their leading coefficients are all equal to $\alpha_{n-1} = (-1)^{n-1}$), condition (25) obviously implies condition (20), thus proving our claim. See Fig. 8 for an illustration.

A.4 Non-binary fragmentation modes are dominated by binary fragmentation modes

For any fitness landscape, binary group splitting achieves a larger growth rate than splitting into more than two offspring groups. To prove this, consider positive integers m, j, k such that $m > j + k$, an arbitrary partition $\tau \vdash m - (j+k)$, and the following three deterministic fragmentation modes:

1. $\kappa_1 = j + k + \tau \vdash m$, whereby a complex of size m fragments into one complex of size j, one complex of size k and a number of offspring complexes given by partition τ.

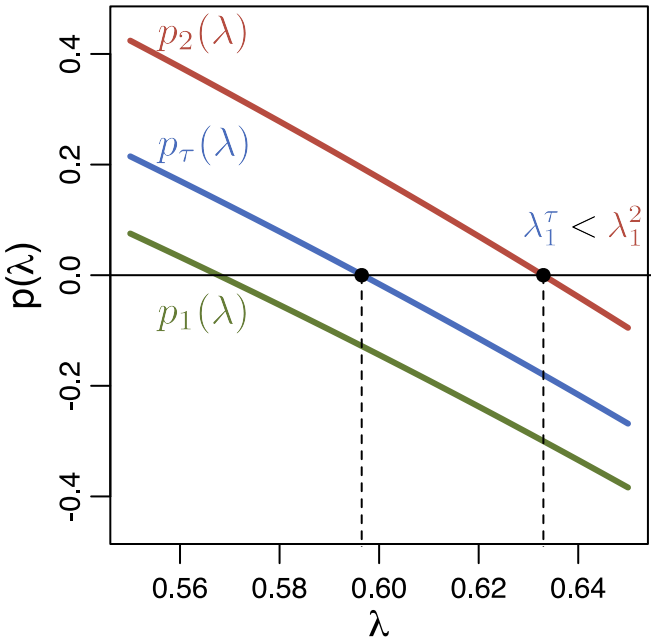

Figure 8: **Population growth rate λ_1 is quasiconvex.** Consider two fragmentation modes $\mathbf{q}_1$ and $\mathbf{q}_2$ which differ only in the probabilities of fragmentation patterns at a single size j. Then, for any $0 \leq \tau \leq 1$ and corresponding fragmentation mode $\mathbf{q}_\tau = \tau\mathbf{q}_1 + (1-\tau)\mathbf{q}_2$, the polynomials $p(\lambda)$ given by Eq. (21) satisfy either $p_1(\lambda) \leq p_\tau(\lambda) \leq p_2(\lambda)$ or $p_2(\lambda) \leq p_\tau(\lambda) \leq p_1(\lambda)$. Thus, $\mathbf{q}_\tau$ leads to a lower growth rate than either $\mathbf{q}_1$ or $\mathbf{q}_2$, i.e., either $\lambda_1^\tau \leq \lambda_1^1$, or $\lambda_1^\tau \leq \lambda_1^2$ holds. Here, $j = 3$, $\mathbf{q}_1 = \{(0.9, 0.1), (\underline{0.5, 0.5, 0}), (0, 0, 0, 1, 0)\}$, $\mathbf{q}_2 = \{(0.9, 0.1), (\underline{0.5, 0, 0.5}), (0, 0, 0, 1, 0)\}$, and $\tau = 0.6$. Note that the life cycle corresponding to $\mathbf{q}_\tau$ is schematically illustrated in Fig. 2*b*. The fitness landscape is given by $b_i = 1/i$, $d_i = 0$ for all i.

2. $\kappa_2 = (j+k) + \tau \vdash m$, whereby a complex of size m fragments into one complex of size $j+k$ and a number of offspring complexes given by partition τ.

3. $\kappa_3 = j + k \vdash (j+k)$, a binary splitting fragmentation mode whereby a complex of size $j+k$ fragments into two offspring complexes: one of size j and one of size k.

Fragmentation mode κ_1 leads to a number of offspring groups equal to

$$n_1 = \sum_{\ell=1}^{m-k-j} \pi_\ell(\tau) + 2,$$

fragmentation mode κ_2 to a number of offspring groups equal to

$$n_2 = \sum_{\ell=1}^{m-k-j} \pi_\ell(\tau) + 1 = n_1 - 1,$$

and fragmentation mode κ_3 to a number of offspring groups equal to two. Denoting by λ_1^i the leading eigenvalue of the projection matrix induced by fragmentation mode κ_i, we can show that, for any fitness landscape, either $\lambda_1^1 \leq \lambda_1^2$ or $\lambda_1^1 \leq \lambda_1^3$ holds. This means that a fragmentation mode with more than two parts is dominated by either a fragmentation mode with one part less or by a fragmentation mode with exactly two parts. By induction, this implies that, for any fitness landscape, the optimal fragmentation mode is always one within the class of binary splitting strategies.

To prove the statement above, let us define the polynomial $p_i(\lambda)$ as the left hand side of Eq. (17) with $\kappa = \kappa_i$, so that λ_1^i is the largest root of $p_i(\lambda)$. We obtain

$$p_1(\lambda) = F_m(\lambda) - \sum_{\ell=1}^{m-j-k} \pi_\ell(\tau) F_\ell(\lambda) - F_j(\lambda) - F_k(\lambda) \tag{26a}$$

$$p_2(\lambda) = F_m(\lambda) - \sum_{\ell=1}^{m-j-k} \pi_\ell(\tau) F_\ell(\lambda) - F_{j+k}(\lambda) \tag{26b}$$

$$p_3(\lambda) = F_{j+k}(\lambda) - F_j(\lambda) - F_k(\lambda). \tag{26c}$$

These polynomials satisfy the following two properties. First,

$$\lim_{\lambda \to \infty} p_i(\lambda) = \infty, \tag{27}$$

as the leading coefficient of the left hand side of Eq. (17) is given by $1/(n! b_1 \dots b_n)$, which is always positive. Second,

$$p_1(\lambda) = p_2(\lambda) + p_3(\lambda). \tag{28}$$

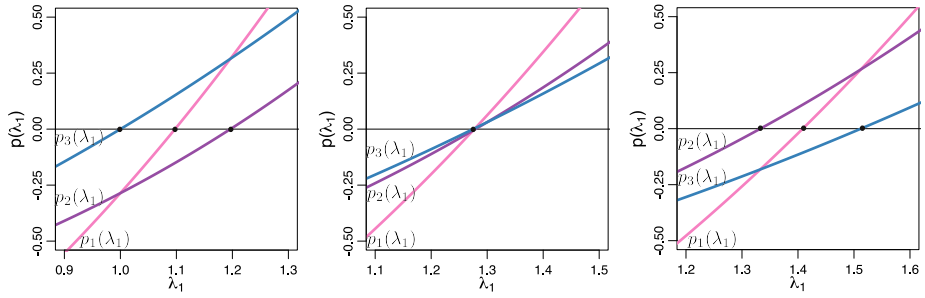

Figure 9: **The population growth rate induced by a fragmentation mode with more than two offspring groups is weakly dominated.** Consider the characteristic polynomials $p_i(\lambda_1)$ for partitions $\kappa_1 = 2+1+1$, $\kappa_2 = 3+1$ and $\kappa_3 = 2+1$. *Left*: Fitness landscape $\mathbf{b} = (1, 1, 1.4)$, $\mathbf{d} = (0, 0, 0)$. Since $p_2(\lambda_1^1) < 0$, κ_1 is dominated by κ_2 ($\lambda_1^1 < \lambda_1^2$ holds). *Center*: Fitness landscape $\mathbf{b} = (1, 2.6 - \sqrt{1.3}, 1.4)$, $\mathbf{d} = (0, 0, 0)$. Since $p_1(\lambda_1^1) = p_1(\lambda_1^2) = p_1(\lambda_1^3)$, κ_1 is weakly dominated by κ_2 ($\lambda_1^1 \leq \lambda_1^2$ holds). *Right*: Fitness landscape $\mathbf{b} = (1, 1.9, 1.4)$, $\mathbf{d} = (0, 0, 0)$. Since $p_3(\lambda_1^1) < 0$, κ_1 is dominated by κ_3 ($\lambda_1^1 < \lambda_1^3$ holds).

Evaluating Eq. (28) at λ_1^1, and since $p_1(\lambda_1^1) = 0$, it then follows that

$$p_2(\lambda_1^1) = -p_3(\lambda_1^1).$$

Hence, only one of the following three scenarios is satisfied: (i) $p_2(\lambda_1^1) < 0 < p_3(\lambda_1^1)$, (ii) $p_2(\lambda_1^1) = p_3(\lambda_1^1) = 0$, or (iii) $p_2(\lambda_1^1) > 0 > p_3(\lambda_1^1)$. If $p_2(\lambda_1^1) < 0 < p_3(\lambda_1^1)$, and by Eq. (27) and Bolzano's theorem, $\lambda_1^1 \leq \lambda_1^2$ holds. Likewise, if $p_2(\lambda_1^1) > 0 > p_3(\lambda_1^1)$, then $\lambda_1^1 \leq \lambda_1^3$ holds. Finally, if $p_2(\lambda_1^1) = p_3(\lambda_1^1) = 0$, then both $\lambda_1^1 \leq \lambda_1^2$ and $\lambda_1^1 \leq \lambda_1^3$ hold. We conclude that either $\lambda_1^1 \leq \lambda_1^2$ or $\lambda_1^1 \leq \lambda_1^3$ must hold. See Fig. 9 for an illustration.

A.5 Optimality maps for $n = 4$

For $n = 4$ there are four deterministic fragmentation modes, denoted by their fragmentation patterns 1+1, 2+1, 2+2, and 3+1. From Eq. (11), their characteristic polynomials are given by

$$1+1: \quad p_{1+1}(\lambda) = F_2(\lambda) - 2F_1(\lambda), \tag{29a}$$

$$2+1: \quad p_{2+1}(\lambda) = F_3(\lambda) - F_2(\lambda) - F_1(\lambda), \tag{29b}$$

$$2+2: \quad p_{2+2}(\lambda) = F_4(\lambda) - 2F_2(\lambda), \tag{29c}$$

$$3+1: \quad p_{3+1}(\lambda) = F_4(\lambda) - F_3(\lambda) - F_1(\lambda). \tag{29d}$$

The optimality maps shown in Fig. 4 were obtained by computing numerically the largest root of the characteristic polynomials and comparing such different values for birth rates (fecundity landscapes) or death rates (viability landscapes). For fecundity landscapes, we tested fitness landscapes of the form $\{\mathbf{b}, \mathbf{d}\} = \{(1, b_2, b_3), (0, 0, 0)\}$ and values b_2 and b_3 taken from a rectangular grid of size 300 by 300 with $b_2 \in [0, 5]$ and $b_3 \in [0, 5]$. For viability landscapes, we tested fitness landscapes of the form $\{\mathbf{b}, \mathbf{d}\} = \{(1, 1, 1), (5, d_2, d_3)\}$ and values d_2 and d_3 taken from a rectangular grid of size 300 by 300 with $d_2 \in [0, 10]$ and $d_3 \in [0, 10]$.

A.6 Costly fragmentation

For costly fragmentation, one cell is lost upon the fragmentation event. In this case the biological reactions are still given by Eqs. (4) and (5). However, under costly fragmentation the sum of sizes of offspring groups is one less than the size of parent group. Therefore, in the reaction describing the group splitting, κ is a partition of j (and not of $j+1$ as it was under the costless fragmentation). Note, that in the reaction describing group growth, κ is still a trivial partition of $j+1$. Thus, for costly fragmentation the set of available outcomes of growth of a group of size j is given by all partitions of j having at least two parts and the trivial partition of $j+1$. For instance, the reactions modeling the birth of units and the growing and fragmentation of groups of size 3 are:

$$\begin{aligned} X_3 &\xrightarrow{3b_3q_{1+1+1}} 3X_1 && 1+1+1 \vdash 3 \\ X_3 &\xrightarrow{3b_3q_{2+1}} X_2 + X_1 && 2+1 \vdash 3 \\ X_3 &\xrightarrow{3b_3q_4} X_4 && 4 \vdash 4. \end{aligned}$$

The combined probability of all outcomes of aggregate growth must be equal to one. In the case of costless fragmentation, this condition has been given by $\sum_{\kappa \vdash j+1} q_\kappa = 1$ for $j = 1, \ldots, n-1$. For costly fragmentation this condition changes to $\sum_{\kappa \vdash j'} q_\kappa = 1$ for $j = 1, \ldots, n-1$, where $j' = j \backslash j \cup (j+1)$ denotes the set of partitions of j with at least two parts together with the trivial partition $(j+1)$. The analogs of Eqs. (6) and (8) are changed accordingly.

Finally, note that for deterministic fragmentation mode, the characteristic equation is still the one derived in Appendix A.1 with the sole exception that, in Eq. (17), $\kappa \vdash m$ (rather than $\kappa \vdash m+1$ as it was the case for costless fragmentation).